European Journal of Medicinal Chemistry 44 (2009) 4121–4127

Contents lists available at ScienceDirect

European Journal of Medicinal Chemistry

journal homepage: http://www.elsevier.com/locate/ejmech

Original article

An efficient steroid pharmacophore-based strategy to identify new aromatase inhibitors

Marco A.C. Neves [a], Teresa C.P. Dinis [b], Giorgio Colombo [c,*], M. Luisa Sá e Melo [a,**]

[a] Centro de Estudos Farmacêuticos, Lab. Química Farmacêutica, Faculdade de Farmácia, Universidade de Coimbra, 3000-548 Coimbra, Portugal
[b] Centro de Neurociências, Lab. Bioquímica, Faculdade de Farmácia, Universidade de Coimbra, 3000-548 Coimbra, Portugal
[c] Istituto di Chimica del Riconoscimento Molecolare, CNR, 20131 Milano, Italy

ARTICLE INFO

Article history:
Received 20 November 2008
Accepted 7 May 2009
Available online 19 May 2009

Keywords:
Pharmacophore modeling
Virtual screening
Aromatase inhibitors
Breast cancer

ABSTRACT

Aromatase, an enzyme involved in the conversion of androgens into estrogens, is an important target for the endocrine treatment of breast cancer. Aromatase inhibition is usually achieved with steroids structurally related to the substrate of catalysis or, alternatively, with azole non-steroid compounds. Substituted androstenedione derivatives with Δ^1, Δ^6 and $\Delta^{1,6}$ unsaturations and 6-alkyl/6-phenyl aliphatic substitutions, are among the most potent steroid aromatase inhibitors known to date. In this paper we have combined the common pharmacophoric and shape features of these molecules into a new pharmacophore model, useful for virtual screening of large compound databases. Small subsets of the best fitting anti-aromatase candidates were extracted from the NCI database and experimentally tested on an in vitro assay with human placental aromatase. New potent aromatase inhibitors were identified such as compounds **8** and **14**. Considering the lack of a crystal structure for the aromatase enzyme, this ligand-based method is a valuable tool for the virtual screening of new aromatase inhibitors.

1. Introduction

Estrogen deprivation is an effective approach for the endocrine treatment of hormone sensitive breast cancer in postmenopausal women. Aromatase, the enzyme responsible for the conversion of androgens into estrogens, is therefore an important pharmacological target [1]. The aromatization reaction is a three-step transformation involving two hydroxylations at the 19-methyl group of androstenedione and testosterone, and a final oxidative decarbonylation. Each reaction consumes a single mole of molecular oxygen and NADPH [2].

Since androstenedione is the preferred substrate for the enzyme [3], the initial development of aromatase inhibitors was focused on this basic scaffold, substituted at several positions. Most of these molecules are competitive inhibitors and bind to the same active site cavity as the natural substrate [4]. Formestane and exemestane, second and third generation aromatase inhibitors, are successful examples of steroid aromatase inhibitors developed with this approach. Indeed, both compounds have been approved for clinical use [5,6]. Other examples of potent inhibitors include androstenedione derivatives with Δ^1, Δ^6 and $\Delta^{1,6}$ unsaturations and 6-*n*-alkyl or 6-*n*-phenyl aliphatic substitutions [7–10]. These compounds highlighted the presence of a hydrophobic pocket close to the C6 position of the steroid nucleus. The length and shape of this substitution were found to be critically important to the activity [11].

Besides competitive aromatase binding, several steroid aromatase inhibitors are converted by the enzyme into reactive intermediates, which are able to cause time-dependent inactivation. These compounds are known as mechanism-based inactivators. The activation step is triggered during a normal catalytic process and depends on the presence of NADPH. Typically, a reactive electrophilic intermediate is formed and immediately reacts with a nucleophilic residue within the active site [12].

Although a crystallographic 3D structure of the aromatase enzyme is still not available, several X-ray structures of homologous mammalian and human cytochrome P450 enzymes [13–16] have been used as templates to build homology models [17–19]. Key atomic details that ultimately determine molecular interactions were identified in structure-based studies and used in the rational design of new aromatase inhibitors [20–22]. Despite clear advances in the

Abbreviations: AG, aminoglutethimide; ESP, electrostatic surface potential; HBA, hydrogen bond acceptor; HOMO, highest occupied molecular orbital; HYD, hydrophobic group; LUMO, lowest unoccupied molecular orbital; NCI, National Cancer Institute; PSA, polar surface area; RMSD, root mean square deviation; VS, virtual screening.

* Corresponding author. Tel.: +39 0228500031; fax: +39 0228901239.
** Corresponding author. Tel.: +351 239488475; fax: +351 239488471.
E-mail addresses: g.colombo@icrm.cnr.it (G. Colombo), samelo@ci.uc.pt (M.L. Sá e Melo).

0223-5234/$ – see front matter © 2009 Elsevier Masson SAS. All rights reserved.
doi:10.1016/j.ejmech.2009.05.003

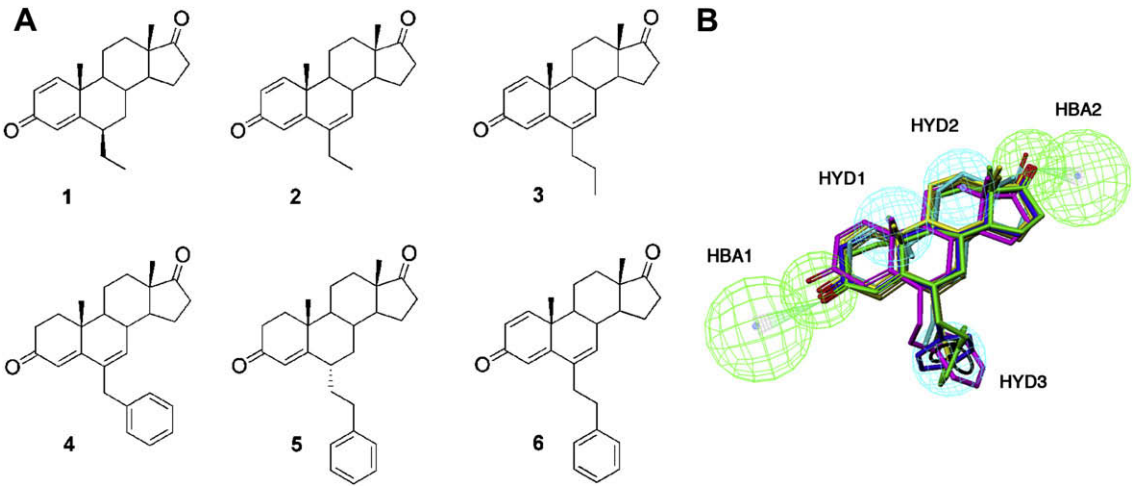

Fig. 1. A) Training set of C6-substituted steroid aromatase inhibitors used for the common-features pharmacophore model generation [7–10]. B) Common-features pharmacophore model of C6-substituted steroid aromatase inhibitors. The STR-HYP pharmacophoric query had five features: two hydrogen bond acceptors (HBA1 and HBA2, green) and three hydrophobic groups (HYD1, HYD2 and HYD3, cyan). The training set inhibitors (**1**, cyan, **2**, brown, **3**, yellow, **4**, blue, **5**, green, **6**, purple) are represented at the best fit alignment to the model. (For interpretation of the references to colour in figure legends, the reader is refered to the web version of this article).

overall quality of aromatase homology models, their usefulness in ligand–protein high throughput docking experiments of large compound databases remains to be demonstrated. On the other hand, ligand-based pharmacophore models such as 3D-QSAR CoMFA developed for several classes of aromatase inhibitors, led to the design of very potent molecules [23–26], and a recent study by Langer and coworkers highlighted the value of pharmacophore models in virtual screening of large electronic compound databases, using a model derived from potent non-steroid aromatase inhibitors [27].

In this work, we have summarized information about C6-substituted androstenedione derivatives, potent steroid aromatase inhibitors, into a ligand-based strategy to identify new anti-aromatase hits. A pharmacophore model recapitulating the most essential structural and functional features linked to activity was built and used to screen the NCI database. The most fitted hits were evaluated experimentally and new potent aromatase inhibitors were identified.

2. Results and discussion

2.1. Pharmacophore modeling

Androstenedione derivatives are among the most potent steroid aromatase inhibitors found to date. In particular, it has been postulated that *n*-alkyl and *n*-phenyl aliphatic groups linked at position C6 increase the anti-aromatase activity due to the presence of a hydrophobic cavity at the enzyme binding site. In this sense, we have used a training set of potent C6-substituted androstenedione derivatives reported in the literature [7–10] (Fig. 1A), namely, 6β-ethylandrosta-1,4-diene-3,17-dione (**1**), 6-ethylandrosta-1,4,6-triene-3,17-dione (**2**), 6-*n*-propylandrosta-1,4,6-triene-3,17-dione (**3**), 6-benzylandrosta-4,6-diene-3,17-dione (**4**), 6α-phenethylandrost-4-ene-3,17-dione (**5**) and 6-phenethylandrosta-1,4,6-triene-3,17-dione (**6**), to derive a common-features pharmacophore model using the HipHop [28] algorithm of the Catalyst software [29]. Briefly, the program identifies chemical features common to a training set of active compounds and generates hypotheses for their activity. These hypotheses are spatial dispositions of pharmacophoric points providing the compounds' relative alignment in the binding site of the enzyme. Each point accounts for an important chemical feature, such as hydrogen bond donors/acceptors, hydrophobic groups, negative/positive ionizable groups and aromatics. Due to the basic structures of the compounds used, hydrogen bond acceptors (HBA) and hydrophobic groups (HYD) were selected for the common-features alignment procedure. Besides its strong potency, this training set of molecules was chosen in order to account for the effect of different lengths, shapes and volumes of the hydrophobic moiety at C6, as well as its stereochemistry in relation to the steroid framework.

Ten different pharmacophore hypotheses were automatically generated by the Catalyst software, with four or five pharmacophore features and alignment scores ranging from 54 to 66. The HipHop algorithm used in this study scores each alignment based on the degree of superimposition of all training set compounds, as well as its estimated rarity [30]. The top ranked solutions had two HBA groups and three HYD moieties, whereas less ranked solutions had only two acceptors and two hydrophobic groups. Visual inspection of the training set molecules aligned to the top ranked solution, STR-HYP (Fig. 1B), revealed that the two hydrogen bond acceptors matched the 3-oxo (HBA1) and the 17-oxo (HBA2) groups. One of the hydrophobic groups, HYD1, superimposes the 19-methyl and the A–B ring junction, HYD2 matches ring C and the 18-methyl, and the third apolar feature, HYD3, is related to the hydrophobic moiety linked at C6. Due to the rigid nature of the steroid scaffold, most of the common-features solutions were very similar to the top ranked pharmacophore model, with slight differences in the projection vectors of HBA1 and HBA2 (the location of hypothetical hydrogen bond donors) and the positioning of HYD3. The top ranked solution was therefore selected for the following steps.

Table 1
NCI database screening results.

Hypothesis	Hits
STR-HYP	16 212
STR-HYP + Shape[a]	2189
STR-HYP + Shape + Filtering[b]	1462
Visual inspection	19

[a] Compound **5** was converted into a shape query and combined with the initial hypothesis. The minimum similarity tolerance was set to 0.5.
[b] Filters applied: Lipinski Rule of Five, rotatable bonds ≤ 8, PSA < 150.

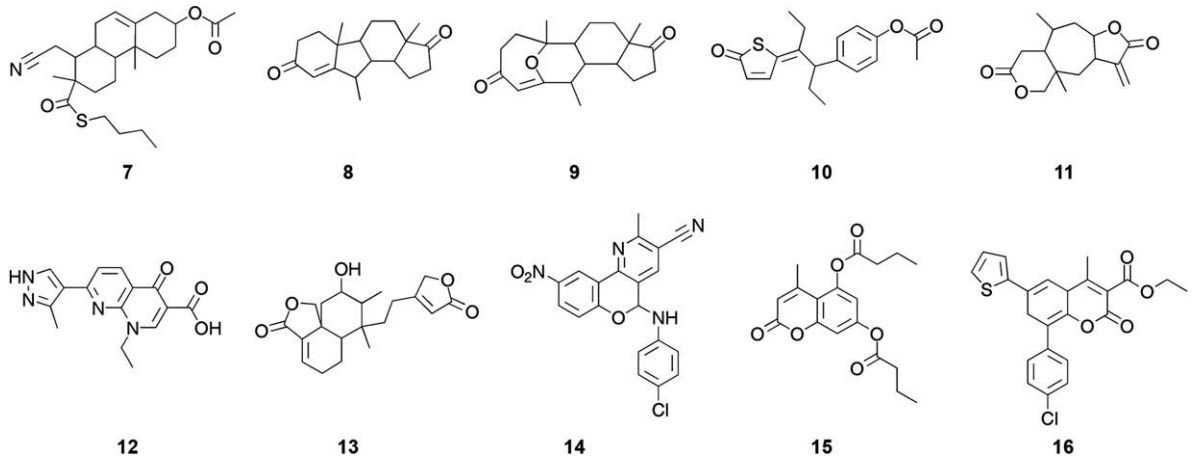

Fig. 2. NCI database hits selected based on the STR-HYP + Shape pharmacophore model.

Cytochrome P450 enzymes have an inner binding cavity accessible from the outside through one or more ligand channels [31]. Therefore, in order to bind to the active site, aromatase inhibitors must have appropriate shape and volume. A set of inclusion volumes based on the shape of compound **5** were applied to STR-HYP, and the steric tolerance was adjusted to allow good shape complementarity with the training set molecules. A new pharmacophore model combining pharmacophoric and shape features was obtained (STR-HYP + Shape).

2.2. Virtual screening

The NCI open chemical repository collection is a large library of synthetic and natural compounds, with more than 260 000 different structures [32]. This library has been used to screen, both in vitro and in vivo, for new anti-cancer and anti-viral agents, with the goal of identifying and evaluating novel chemical leads and their underlying biological mechanisms of action. The electronic version of the NCI repository (NCI database) was downloaded from the ZINC website [33] and converted into a multiconformer database using the catDB utility program of the Catalyst software [29].

An initial virtual screening (VS) run with the STR-HYP pharmacophore model identified 16 212 hits (5.6% of the database, Table 1), and the modified pharmacophore hypothesis, STR-HYP + Shape, yielded 2189 hits (0.8% of total number of compounds, Table 1). Most of the molecules excluded, based on shape features, are expected to be false positives due to the presence of protruding groups that might clash with aromatase binding site residues.

Furthermore, in order to increase the "drug-likeness" of the new anti-aromatase candidates, several filters were applied, namely a Lipinski Rule of Five filter [34], and filters based on the maximum number of rotatable bonds (not more than 8) and polar surface area (PSA < 150). This procedure reduced the number of compounds to 1462 (0.5% of the database, Table 1). The molecules were then superimposed with the pharmacophore model and visually inspected, 19 of them being selected based on a good root mean square deviation (RMSD) fit to the model. Of these, 10 were available from the NCI database (Fig. 2) and were obtained for experimental evaluation.

Before performing the biochemical evaluation, the hits were inspected on a large electronic collection of organic chemistry (CrossFire Beilstein) using the MDL CrossFire Commander [35]. Additional searches were performed using the PubChem Compound database [36], a publicly available resource with chemical and biological information of small molecules, including results from NCI anti-cancer drug screenings. It was found that none of them had been previously tested experimentally as aromatase inhibitor.

2.3. Biochemical evaluation

The compounds selected using our ligand-based VS strategy were biochemically evaluated for the ability to inhibit the enzyme aromatase. The molecules were initially screened at 10 μM and 100 μM concentrations, followed by a full concentration–response study, allowing the determination of the half-maximal inhibitory concentration (IC_{50}) reported in Table 2. Formestane and aminoglutethimide (AG), second and first generation aromatase inhibitors, were also tested, in the same assay conditions, as reference compounds.

Table 2
Aromatase inhibition activity of NCI hits selected based on the STR-HYP + Shape pharmacophore model. Aminoglutethimide and formestane were tested as reference aromatase inhibitors.

Compound id	NCI code	IC_{50} (μM)[a]	Inhibition at 100 μM
7	NSC76982	–	21%[b]
8	NSC93358	0.274 ± 0.004	–
9	NSC94891	9.8 ± 0.2	–
10	NSC122427	15.5 ± 0.1	–
11	NSC136718	–	N.O.[c]
12	NSC302379	–	N.O.[c]
13	NSC383467	126 ± 15	–
14	NSC613604	0.678 ± 0.007	–
15	NSC688803	176 ± 3	–
16	NSC692587	–	26%
Aminoglutethimide	–	10.0 ± 0.1	–
Formestane	–	0.092 ± 0.004	–

[a] Results are shown as the mean ± SEM of three independent experiments.
[b] Inhibition at 30 μM.
[c] Inhibition was not observed at concentrations ≤100 μM.

Table 3
Enzyme kinetic parameters for compounds **8** and **14**, and type of aromatase inhibition, based on a kinetic and time-dependent inactivation procedure.

Compound id	K_i (μM)[a]	Type of inhibition[a]	K_I (μM)[b]	k_{inact} (min^{-1})[b]
8	0.266 ± 0.002	Competitive	N.O.[c]	N.O.[c]
14	0.385 ± 0.008	Competitive	21.4 ± 1.0	0.608 ± 0.044

[a] Apparent inhibition constants (K_i) were calculated by a nonlinear regression analysis using the Michaelis–Menten equation, and the type of inhibition was determined by a Lineweaver–Burk plot.
[b] K_I and k_{inact} were obtained by a Kitz–Wilson plot.
[c] Inactivation was not observed at concentrations ≤2 μM.

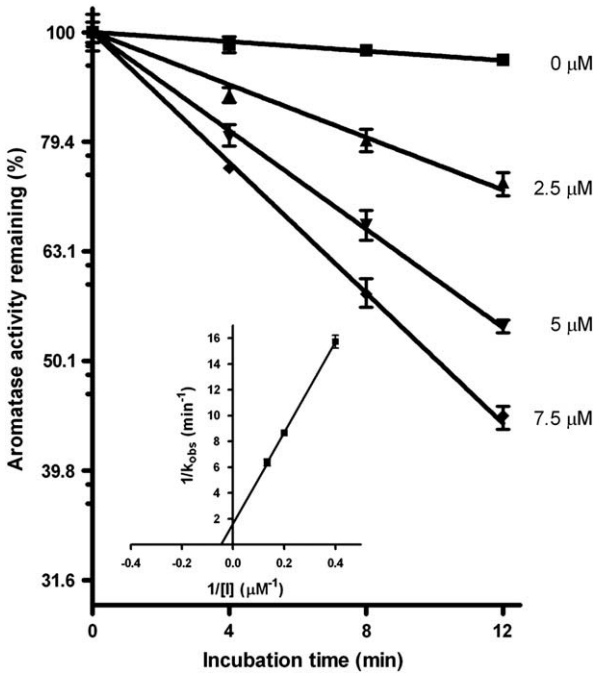

Fig. 3. Time- and concentration-dependent inactivation of human placental aromatase by compound **14** in the presence of NADPH. The concentrations of inhibitor used were 0 μM (■), 2.5 μM (▲), 5 μM (▼) and 7.5 μM (◆). A Kitz–Wilson plot of the same data is shown in the inset. Each point represents the mean of three independent assays and the vertical bars, the standard error of the mean (SEM).

Most of the compounds selected showed anti-aromatase activity in the assay conditions used (Table 2). Compounds **7**, **13**, **15** and **16** are weak aromatase inhibitors with IC_{50} higher than 100 μM. Compounds **9** ($IC_{50} = 9.8$ μM) and **10** ($IC_{50} = 15.5$ μM), have anti-aromatase potencies comparable to the first generation aromatase inhibitor tested, aminoglutethimide ($IC_{50} = 10.0$ μM), and, more interestingly, compounds **8** and **14** have an IC_{50} in the nanomolar range. Compound **8** ($IC_{50} = 0.274$ μM) is 36 times more active than aminoglutethimide, and compound **14** ($IC_{50} = 0.678$ μM) 15 times more potent than AG. However, these two molecules are less active than formestane ($IC_{50} = 0.092$ μM), the second generation aromatase inhibitor tested.

Kinetic analysis of the enzyme activity was also performed. The kinetic constants, Michaelis–Menten constant ($K_m = 0.094$ μM) and maximum velocity of catalysis ($V_{max} = 163.7$ pmol of substrate min^{-1} mg^{-1} of protein) were calculated under initial velocity conditions. The type of inhibition was characterized using a Lineweaver–Burk plot. As expected, the most potent aromatase inhibitors (compounds **8**, $K_i = 0.266$ μM, and **14**, $K_i = 0.385$ μM), inhibited the enzyme in a competitive manner (Table 3).

Compounds **8** and **14** were further tested for their ability to cause time-dependent inactivation of aromatase. Compound **14**, but not compound **8**, was able to inactivate the enzyme in the presence of NADPH, with a pseudo first order kinetics during the first 12 min of incubation (Fig. 3). Kitz–Wilson analysis [37] of the results obtained, gave a k_{inact} of 0.608 min^{-1} and K_I of 21.4 μM. Since the K_i observed from the competition kinetics is lower than the K_I obtained from the inactivation experiments, this suggests that the covalent binding of the inhibitor to the active site of the enzyme is the rate-limiting step of the inactivation. On the other hand, addition of substrate androstenedione in excess prevented inactivation (Fig. 4A), as well as not including NADPH in the medium (Fig. 4B). This suggests that the inhibitor acts at or near the active site of aromatase, and, since NADPH was essential for the time-dependent aromatase activity loss by compound **14**, that the inhibitor transformation into a reactive intermediate depends on enzyme catalysis. Furthermore, the nucleophilic trapping agent L-cysteine did not prevent enzyme inactivation to a significant extent (Fig. 4C), suggesting a covalent bond formation at the active site, between aromatase and the reactive electrophilic intermediate, therefore preventing diffusion of the activated inhibitor to the surrounding media.

2.4. Stereoelectronic characterization

The strong anti-aromatase activity of compound **8**, a B-nor steroid with similar hydrophobic core compared to the substrate androstenedione, prompted us to further evaluate the molecular geometry and electronic properties of these structures using high

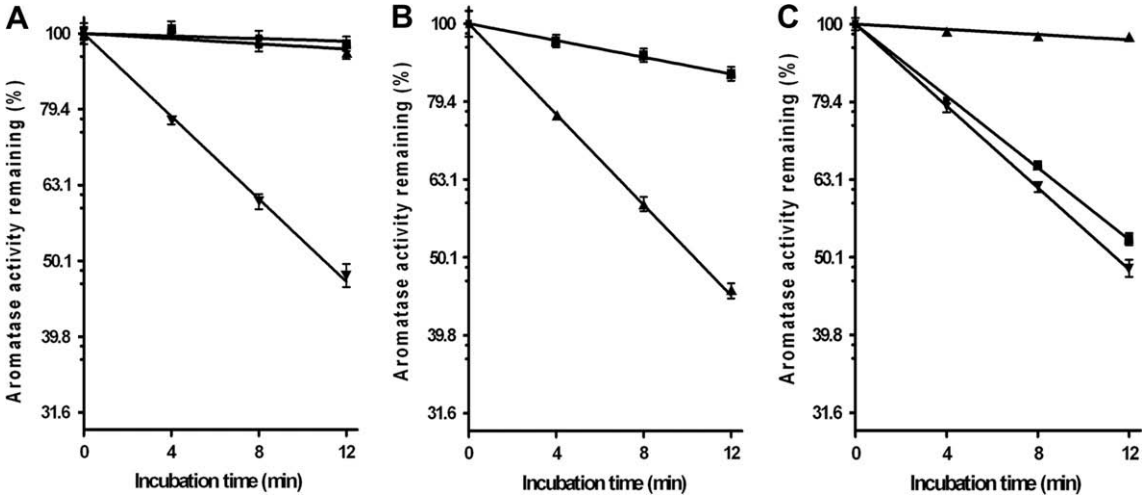

Fig. 4. Effect of androstenedione (A), NADPH (B) and L-cysteine (C) on the time-dependent inactivation of human placental aromatase by compound **14**. A) 7.5 μM of androstenedione was incubated with (■) or without (▲) 7.5 μM of inhibitor. Incubations of 7.5 μM of inhibitor without androstenedione (▼) were also performed. B) 7.5 μM of inhibitor was incubated with (▲) or without (■) NADPH. C) 0.5 mM of L-cysteine was incubated with (■) or without (▲) 7.5 μM of inhibitor. Incubations of 7.5 μM of inhibitor without L-cysteine (▼) were also performed. Each point represents the mean of three independent assays and the vertical bars, the standard error of the mean.

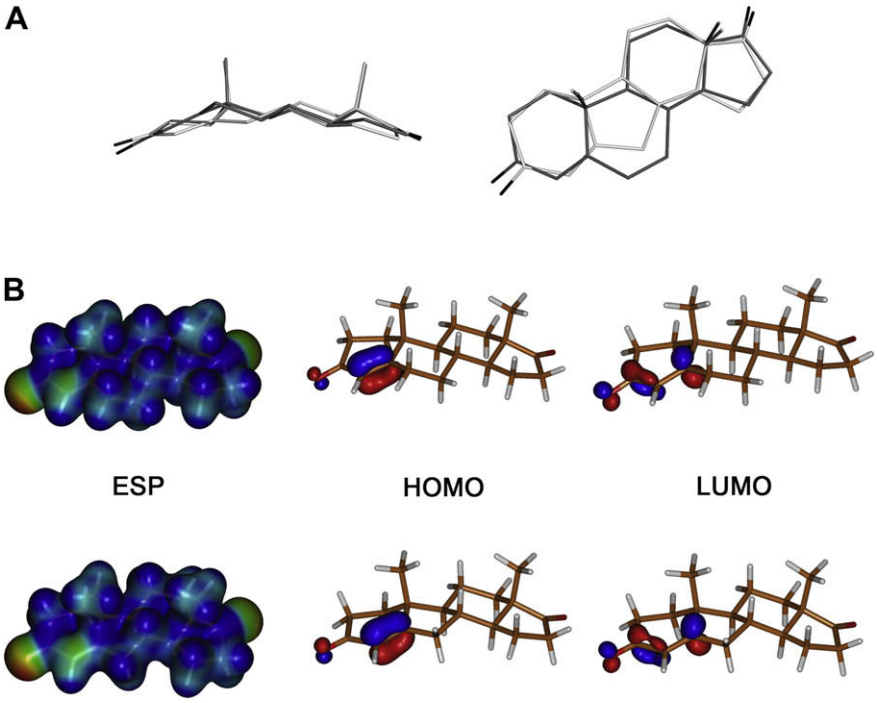

Fig. 5. A) Superimposition of the minimized structures of androstenedione (grey) and B-nor-androstenedione (white) at the ab initio HF/6-31G** level. The molecules were superimposed based on RMSD of carbon atoms at the A, C and D rings, and represented on a side (right) and top view (left). B) Electrostatic surface potential (ESP), HOMO and LUMO valence orbitals derived for androstenedione (top) and B-nor-androstenedione (bottom). The ESP was mapped on the 0.02 e/Å^3 electron density isocontour derived from ab initio HF/6-31G** calculations ($V = 0.1$ eV, blue; $V = -0.1$ eV, red). The HOMO and LUMO are represented at an orbital amplitude of 0.1 (blue) and −0.1 (red). (For interpretation of the references to colour in figure legends, the reader is refered to the web version of this article).

level ab initio quantum chemistry methods. It was found that the geometries of androstenedione and its B-nor derivative are very superimposable, with an RMSD of 0.31 Å based on pairwise alignment of the A, C and D ring carbons (Fig. 5A). Furthermore, the distances between the hydrogen bond acceptor groups, an important pharmacophoric feature in our model, are very similar (10.44 Å in androstenedione and 10.38 Å in the B-nor derivative). Slight differences were however identified, namely the shape and size of the B ring, and the location of the acceptor linked to the ring A. The B ring of the nor-steroid, a cyclopentane, adopts an envelope conformation which is less bulky than the cyclohexane chair in androstenedione. The 3-oxo groups are located 0.63 Å apart based on our superimposition.

Electronic properties of the molecules were also calculated, namely the electrostatic surface potential (ESP) and the valence orbitals, i.e. the highest occupied molecular orbital (HOMO) and the lowest unoccupied molecular orbital (LUMO). These properties are similar in both compounds (Fig. 5B). Negative potential was found in both carbonyls and along the O=C3–C4=C5 conjugation due to π electron delocalization. The HOMO and the LUMO are located at the A-ring, on the delocalized system. Therefore, both compounds are expected to share a similar aromatase recognition mechanism and reactivity.

3. Conclusions

In this paper we have built a new pharmacophore model for an important class of aromatase inhibitors and used it in a virtual screening study for new anti-aromatase hits. Previous knowledge on the binding determinants of C6-substituted androstenedione derivatives to the aromatase active site was essential to this ligand-based approach. A hydrophobic pocket close to the C6 of steroid inhibitors was explored to improve the binding affinity of the new anti-aromatase candidates. Therefore, the combination of essential pharmacophoric features with steric restrictions and "drug-likeness" filters allowed the isolation of a small subset, enriched in strong aromatase inhibitors, from the large NCI database.

The screening methodology was validated experimentally by testing some of the most promising VS hits on an in vitro assay, and new potent aromatase inhibitors were found. 6-Methyl-B-nor-androstenedione (**8**) was one of the most interesting compounds identified, with a low nanomolar IC_{50} and a competitive mechanism of inhibition. The strong anti-aromatase potency was rationalized based on structural and physicochemical similarities between the B-nor-androstenedione scaffold and the natural substrate of the enzyme. To the best of our knowledge, this is the first report of B-nor-androgens as aromatase inhibitors. These compounds represent an important new structural class of anti-aromatase agents and should be further optimized. Compound **14** was another interesting molecule identified, combining strong competitive inhibition properties with mechanism-based inactivation of the enzyme. Compounds **9** and **10** had anti-aromatase potencies comparable to aminoglutethimide.

The value of experimentally validated virtual screening approaches of large compound databases relies on fast and affordable identification of new hit compounds for particular targets of interest. However, hits identified with such approaches are usually non-optimized structures. Therefore, it is not surprising that the new aromatase inhibitors reported in this study are less potent than formestane. Nonetheless, starting with a training set of compounds from a single class, we were able to increase the chemical diversity of aromatase inhibitors, identifying interesting new scaffolds which can be further explored by lead optimization.

In conclusion, we have described and validated a new ligand-based VS methodology for new aromatase inhibitors based on a pharmacophore model with common-features of steroid inhibitors. The screening of a large compound database was very fast and new potent and chemically diverse aromatase inhibitors could be

identified. Moreover, this methodology has a broader application for a large variety of compound databases.

4. Computational and experimental methods

4.1. Materials and general methods

The NCI selected compounds were obtained from the Drug Synthesis and Chemistry Branch, Developmental Therapeutics Program, Division of Cancer Treatment and Diagnosis of the National Cancer Institute. DL-Aminoglutethimide, androstenedione, formestane and NADPH were purchased from Sigma–Aldrich (St. Louis, MO, U.S.A.). The [1β-^{3}H] androstenedione (specific activity of 25.3 Ci/mmol) and the liquid scintillation cocktail Optiphase Hisafe 2 were purchased from PerkinElmer (Boston, MA, U.S.A.). Radioactive samples were counted on a Packard Tri-Carb 2900 TR Liquid Scintillation Analyzer. All the other reagents were of adequate grade for biochemical analysis.

4.2. Pharmacophore modeling

Pharmacophore design was performed using the Catalyst software [29]. The aromatase inhibitors were initially submitted to the catDB utility program and a conformational search with internal energy minimization was performed using the best quality generation type. A maximum of 250 conformers were saved within an energy window of 20 kcal/mol above the global minimum. The HipHop algorithm [28] of Catalyst was used for the common-features pharmacophore model, using hydrophobic and hydrogen bond acceptor functions. The "Principal" value was set to 2 for molecule **3** (all features in the molecule were considered to build the pharmacophore model) and 1 for the other compounds (at least one mapping for each generated hypothesis was found). The "maximum omitted features" value was set to 1 for all the molecules (all but one feature was forced to map) and default settings were used for the other options. A similarity tolerance of 0.5 was used in the shape query. This value was chosen in order to match all training set molecules.

4.3. Virtual screening

The NCI database was downloaded from the 2007 release of the ZINC database [33] and converted into a multiconformer Catalyst database using the "FAST" conformational analysis model of the catDB utility program. A maximum of 100 conformations were generated and saved for each molecule. Pharmacophore searches were performed with "fast flexible database search" settings.

Instant JChem [38] was used for management, search and prediction of molecular descriptors for the NCI hits. A Lipinski Rule of Five [34] filter was applied (molecular weight under 500 g/mol, not more than 5 hydrogen bond donors, not more than 10 hydrogen bond acceptors and calculated partition coefficient, *c* log *P*, less than 5), as well as a filter based on the maximum number of rotatable bonds (not more than 8) and the maximum PSA (less than 150).

4.4. Human placental isolation

Human term placental microsomes were obtained by differential centrifugation, according to the method described by Ryan [39], and were used as a source of aromatase. The microsomes were obtained by differential centrifugation and were resuspended in a buffer containing sodium phosphate (0.1 M), sucrose (0.25 M), glycerol (20%) and dithiothreitol (0.5 mM), pH 7.4, and stored in aliquots at −80 °C until needed.

Microsomal protein content was determined by the biuret method using bovine serum albumin as standard.

4.5. Concentration–response and kinetic studies

Aromatase activity was evaluated according to the method described by Siiteri and Thompson [40]. The concentration–response and initial velocity experiments were performed as previously described [20,41]. Briefly, microsomal protein (30 μg), [1β-^{3}H] androstenedione (6.6×10^5 dpm) and NADPH (270 μM) were used for the concentration–response experiment with an incubation time of 20 min. The molecules in study were initially tested at 10 μM and 100 μM concentrations, followed by a full concentration–response study with at least 8 concentrations ranging from 0.01 μM to 160 μM. For the initial velocity study the concentration of [1β-^{3}H] androstenedione was varied from 7.5 to 100 nM and the incubation time was set to 5 min. Three different concentrations of each inhibitor were tested. The tritiated water formed during the conversion of the tritiated substrate, [1β-^{3}H] androstenedione, to estrone was quantified by liquid scintillation counting. Each assay was performed three times in duplicate and the results were treated by nonlinear regression analysis.

4.6. Time-dependent inactivation assay

Several concentrations of compounds **8** and **14** (up to ca. 10 times the IC_{50}) were incubated at 37 °C in a medium containing sodium phosphate buffer (67 mM), pH 7.5, microsomal protein (300 μg) and NADPH (900 μM), in a final volume of 500 μL. Aliquots (50 μL) were removed in duplicate at several times (0, 4, 8 and 12 min), and immediately diluted in sodium phosphate buffer (67 mM), pH 7.5, [1β-^{3}H] androstenedione (6.6×10^5 dpm) and NADPH (270 μM) in a final volume of 500 μL. The mixture was then incubated at 37 °C for 20 min, and the extent of the aromatization reaction was determined by liquid scintillation counting as described previously. Each assay was performed three times. First order inactivation constants (k_{obs}), at each inactivator concentration, were obtained from the slope of linear regressions of log aromatase activity remaining versus incubation time plots, multiplied by 2.303. The K_I and k_{inact} were determined from the slope and *y* intercept of a Kitz–Wilson plot [37], respectively. Inactivation studies in the absence of NADPH were performed in the same manner, but NADPH was omitted in the initial incubation. For the same studies in the presence of androstenedione or L-cysteine, the substrate (7.5 μM) or L-cysteine (0.5 mM) was included in the initial incubation.

4.7. Ab initio calculation details

The minimum energy conformations and electronic properties were determined by ab initio quantum chemistry calculations. Building blocks from the standard libraries of MAESTRO [42] were used to generate the initial geometry for the molecules in study, followed by a conformational search with the Systematic Unbounded Multiple Minimum (SUMM) [43] routine implemented in MACROMODEL v8.1 [44], using the Merck Molecular Force Field (MMFF) [45] and the Generalized Born equation/Surface Area (GB/SA) continuum solvation model [46] with parameters for water (dielectric constant ε of 78). The molecular mechanics geometries were further optimized with Gaussian 98 [47] using a split-valence basis set with polarization d-orbitals added to heavy atoms and polarization p-orbitals added to hydrogens (HF/6-31G**).

The optimized geometries were used to calculate electronic properties, namely the total density, ESP, HOMO and LUMO. Contour surfaces were represented using Molden v4.6 software [48].

Acknowledgements

We thank Fundação para a Ciência e a Tecnologia (FCT) through POCI for financial support and the Drug Synthesis and Chemistry Branch, Developmental Therapeutics Program, Division of Cancer Treatment and Diagnosis of the National Cancer Institute for kindly providing the compounds screened in this study. We also acknowledge the Maternity Daniel de Matos, Coimbra, Portugal for providing the human placenta. M. A. C. Neves thanks FCT for a Ph.D. grant (SFRH/BD/17624/2004).

References

[1] I.E. Smith, M. Dowsett, N. Engl. J. Med. 348 (2003) 2431–2442.
[2] B. Meunier, S.P. de Visser, S. Shaik, Chem. Rev. 104 (2004) 3947–3980.
[3] Y. Shimizu, C. Yarborough, Y. Osawa, J. Steroid Biochem. Mol. Biol. 44 (1993) 651–656.
[4] R.W. Brueggemeier, Breast Cancer Res. Treat. 30 (1994) 31–42.
[5] R.C. Coombes, E. Hall, L.J. Gibson, R. Paridaens, J. Jassem, T. Delozier, S.E. Jones, I. Alvarez, G. Bertelli, O. Ortmann, A.S. Coates, E. Bajetta, D. Dodwell, R.E. Coleman, L.J. Fallowfield, E. Mickiewicz, J. Andersen, P.E. Lonning, G. Cocconi, A. Stewart, N. Stuart, C.F. Snowdon, M. Carpentieri, G. Massimini, J.M. Bliss, N. Engl. J. Med. 350 (2004) 1081–1092.
[6] P.E. Goss, T.J. Powles, M. Dowsett, G. Hutchison, A.M.H. Brodie, J.C. Gazet, R.C. Coombes, Cancer Res. 46 (1986) 4823–4826.
[7] M. Numazawa, M. Oshibe, S. Yamaguchi, M. Tachibana, J. Med. Chem. 39 (1996) 1033–1038.
[8] M. Numazawa, M. Oshibe, S. Yamaguchi, Steroids 62 (1997) 595–602.
[9] M. Numazawa, S. Yamaguchi, J. Steroid Biochem. Mol. Biol. 67 (1998) 41–48.
[10] M. Numazawa, S. Yamaguchi, Steroids 64 (1999) 187–196.
[11] M. Numazawa, M. Shelangouski, M. Nagasaka, Steroids 65 (2000) 871–882.
[12] R.W. Brueggemeier, J.C. Hackett, E.S. Diaz-Cruz, Endocr. Rev. 26 (2005) 331–345.
[13] P. Rowland, F.E. Blaney, M.G. Smyth, J.J. Jones, V.R. Leydon, A.K. Oxbrow, C.J. Lewis, M.G. Tennant, S. Modi, D.S. Eggleston, R.J. Chenery, A.M. Bridges, J. Biol. Chem. 281 (2006) 7614–7622.
[14] P.A. Williams, J. Cosme, V. Sridhar, E.F. Johnson, D.E. Mcree, J. Inorg. Biochem. 81 (2000) 183–190.
[15] P.A. Williams, J. Cosme, A. Ward, H.C. Angova, D.M. Vinkovic, H. Jhoti, Nature 424 (2003) 464–468.
[16] P.A. Williams, J. Cosme, D.M. Vinkovic, A. Ward, H.C. Angove, P.J. Day, C. Vonrhein, I.J. Tickle, H. Jhoti, Science 305 (2004) 683–686.
[17] A.D. Favia, A. Cavalli, M. Masetti, A. Carotti, M. Recanatini, Proteins 62 (2006) 1074–1087.
[18] S. Karkola, H.D. Holtje, K. Wahala, J. Steroid Biochem. Mol. Biol. 105 (2007) 63–70.
[19] C. Loge, M. Le Borgne, P. Marchand, J.M. Robert, G. Le Baut, M. Palzer, R.W. Hartmann, J. Enzyme Inhib. Med. Chem. 20 (2005) 581–585.
[20] M.A.C. Neves, T.C.P. Dinis, G. Colombo, M.L.S. Melo, ChemMedChem 2 (2007) 1750–1762.
[21] M. Cepa, G. Correia-Da-Silva, E.J.T. da Silva, F.M.F. Roleira, Y.Y. Hong, S. Chen, N.A. Teixeira, Biol. Chem. 389 (2008) 1183–1191.
[22] T. Jackson, L.W.L. Woo, M.N. Trusselle, A. Purohit, M.J. Reed, B.V.L. Potter, ChemMedChem 3 (2008) 603–618.
[23] S. Gobbi, A. Cavalli, A. Rampa, F. Belluti, L. Piazzi, A. Paluszcak, R.W. Hartmann, M. Recanatini, A. Bisi, J. Med. Chem. 49 (2006) 4777–4780.
[24] F. Leonetti, A. Favia, A. Rao, R. Aliano, A. Paluszcak, R.W. Hartmann, A. Carotti, J. Med. Chem. 47 (2004) 6792–6803.
[25] M. Recanatini, A. Cavalli, Bioorg. Med. Chem. 6 (1998) 377–388.
[26] A. Cavalli, G. Greco, E. Novellino, M. Recanatini, Bioorg. Med. Chem. 8 (2000) 2771–2780.
[27] D. Schuster, C. Laggner, T.M. Steindl, A. Palusczak, R.W. Hartmann, T. Langer, J. Chem. Inf. Model. 46 (2006) 1301–1311.
[28] O.O. Clement, A.T. Mehl, in: O.F. Güner (Ed.), Pharmacophore Perception, Development, and Use in Drug Design, International University Line, La Jolla, CA, 2000, pp. 69–84.
[29] Catalyst, Release Version 4.11, Accelrys Software Inc, 2007, www.accelrys.com.
[30] D. Barnum, J. Greene, A. Smellie, P. Sprague, J. Chem. Inf. Comput. Sci. 36 (1996) 563–571.
[31] K. Schleinkofer, Sudarko, P.J. Winn, S.K. Ludemann, R.C. Wade, EMBO Rep. 6 (2005) 584–589.
[32] Developmental Therapeutics Program, NCI/NIH, 2008, http://dtp.nci.nih.gov.
[33] J.J. Irwin, B.K. Shoichet, J. Chem. Inf. Model. 45 (2005) 177–182.
[34] C.A. Lipinski, F. Lombardo, B.W. Dominy, P.J. Feeney, Adv. Drug Deliv. Rev. 23 (1997) 3–25.
[35] MDL CrossFire Commander, Release Version 7.0SP2, Elsevier MDL, 2005, www.mdli.com.
[36] PubChem Compound database, 2008, available at: http://www.ncbi.nlm.nih.gov/sites/entrez/.
[37] R. Kitz, I.B. Wilson, J. Biol. Chem. 237 (1962) 3245–3249.
[38] Instant JChem, Release Version 2.0.0, ChemAxon, 2008, www.chemaxon.com.
[39] K.J. Ryan, J. Biol. Chem. 234 (1959) 268–272.
[40] P.K. Siiteri, E.A. Thompson, J. Steroid Biochem. 6 (1975) 317–322.
[41] M.A.C. Neves, T.C.P. Dinis, G. Colombo, M.L.S. Melo, J. Steroid Biochem. Mol. Biol. 110 (2008) 10–17.
[42] MAESTRO, Release Version 8.0.314, Schrodinger, 2008, www.schrodinger.com.
[43] J.M. Goodman, W.C. Still, J. Comput. Chem. 12 (1991) 1110–1117.
[44] F. Mohamadi, N.G.J. Richards, W.C. Guida, R. Liskamp, M. Lipton, C. Caufield, G. Chang, T. Hendrickson, W.C. Still, J. Comput. Chem. 11 (1990) 440–467.
[45] T.A. Halgren, J. Comput. Chem. 17 (1996) 490–519.
[46] W. Clark Still, Anna Tempczyk, Ronald C. Hawley, Thomas Hendrickson, J. Am. Chem. Soc. 112 (1990) 6127–6129.
[47] M.J. Frisch, G.W. Trucks, H.B. Schlegel, G.E. Scuseria, M.A. Robb, J.R. Cheeseman, V.G. Zakrzewski, J.A. Montgomery Jr., R.E. Stratmann, J.C. Burant, S. Dapprich, J.M. Millam, A.D. Daniels, K.N. Kudin, M.C. Strain, O. Farkas, J. Tomasi, V. Barone, M. Cossi, R. Cammi, B. Mennucci, C. Pomelli, C. Adamo, S. Clifford, J. Ochterski, G.A. Petersson, P.Y. Ayala, Q. Cui, K. Morokuma, D.K. Malick, A.D. Rabuck, K. Raghavachari, J.B. Foresman, J. Cioslowski, J.V. Ortiz, A.G. Baboul, B.B. Stefanov, G. Liu, A. Liashenko, P. Piskorz, I. Komaromi, R. Gomperts, R.L. Martin, D.J. Fox, T. Keith, M.A. Al-Laham, C.Y. Peng, A. Nanayakkara, C. Gonzalez, M. Challacombe, P.M.W. Gill, B.G. Johnson, W. Chen, M.W. Wong, J.L. Andres, M. Head-Gordon, E.S. Replogle, J.A. Pople, Gaussian 98, Revision A.7, Gaussian, Inc., Pittsburgh, PA, USA, 1998, www.gaussian.com.
[48] G. Schaftenaar, J.H. Noordik, J. Comput.-Aided Mol. Des. 14 (2000) 123–134.